



OPEN

Annexin A5 prevents amyloid- β -induced toxicity in choroid plexus: implication for Alzheimer's disease

Fernando Bartolome^{1,2,12}✉, Agnieszka Krzyzanowska^{2,12}, Macarena de la Cueva^{1,2}, Consuelo Pascual², Desiree Antequera^{1,2}, Carlos Spuch³, Alberto Villarejo-Galende^{1,2,4}, Alberto Rabano⁵, Juan Fortea^{1,6,7}, Daniel Alcolea^{1,6,7}, Alberto Lleó^{1,6,7}, Isidro Ferrer^{1,8,9}, John Hardy¹⁰, Andrey Y. Abramov¹¹ & Eva Carro^{1,2}✉

In Alzheimer's disease (AD) amyloid- β (A β) deposits may cause impairments in choroid plexus, a specialised brain structure which forms the blood–cerebrospinal fluid (CSF) barrier. We previously carried out a mass proteomic-based study in choroid plexus from AD patients and we found several differentially regulated proteins compared with healthy subjects. One of these proteins, annexin A5, was previously demonstrated implicated in blocking A β -induced cytotoxicity in neuronal cell cultures. Here, we investigated the effects of annexin A5 on A β toxicity in choroid plexus. We used choroid plexus tissue samples and CSF from mild cognitive impairment (MCI) and AD patients to analyse A β accumulation, cell death and annexin A5 levels compared with control subjects. Choroid plexus cell cultures from rats were used to analyse annexin A5 effects on A β -induced cytotoxicity. AD choroid plexus exhibited progressive reduction of annexin A5 levels along with progressive increased A β accumulation and cell death as disease stage was higher. On the other hand, annexin A5 levels in CSF from patients were found progressively increased as the disease stage increased in severity. In choroid plexus primary cultures, A β administration reduced endogenous annexin A5 levels in a time-course dependent manner and simultaneously increased annexin A5 levels in extracellular medium. Annexin A5 addition to choroid plexus cell cultures restored the A β -induced impairments on autophagy flux and apoptosis in a calcium-dependent manner. We propose that annexin A5 would exert a protective role in choroid plexus and this protection is lost as A β accumulates with the disease progression. Then, brain protection against further toxic insults would be jeopardised.

Alzheimer's disease (AD) is a progressive neurodegenerative disorder and the most common cause of dementia in elderly^{1,2}. The imbalance between amyloid- β (A β) peptide generation from amyloid precursor protein³ and clearance, induces its accumulation, aggregation, and deposition in the brain, which is thought to be an early and main pathogenic event in AD^{2,4}. Besides accumulation and production in specific parenchyma areas, such as hippocampus and cortex, and blood vessels⁵, A β also accumulates in choroid plexus^{6,7}. More specifically it was demonstrated that A β may be additionally produced and degraded in choroid plexus along with other brain areas^{8–10}. Choroid plexus is a monolayer of specialised epithelial cells in the brain ventricles forming the blood – cerebrospinal fluid (CSF) barrier. The choroid plexus main function is to produce and secrete CSF (CSF turnover)

¹Networking Biomedical Research Center on Neurodegenerative Diseases (CIBERNED), Madrid, Spain. ²Group of Neurodegenerative Diseases, Hospital 12 de Octubre Research Institute (imas12), Madrid, Spain. ³Neuroscience Translational Group, Galicia Sur Health Research Institute, SERGAS-Universidad de Vigo; CIBERSAM, Vigo, Spain. ⁴Neurology service Hospital Universitario 12 de Octubre, Madrid, Spain. ⁵Department of Neuropathology and Tissue Bank, Unidad de Investigación Proyecto Alzheimer, Fundación CIEN, Instituto de Salud Carlos III, Madrid, Spain. ⁶Memory Unit, Neurology Department, Hospital de la Santa Creu i Sant Pau, Barcelona, Spain. ⁷Institut d'Investigacions Biomediques Sant Pau - Universitat Autònoma de Barcelona, Barcelona, Spain. ⁸IDIBELL-Hospital Universitari de Bellvitge, Hospitalet de Llobregat, Hospitalet de Llobregat, Spain. ⁹Universitat de Barcelona, Hospitalet de Llobregat, Hospitalet de Llobregat, Spain. ¹⁰Department of Neurodegenerative Disease, UCL Queen Square Institute of Neurology, London, United Kingdom. ¹¹Department of Clinical and Movement Neurosciences, UCL Queen Square Institute of Neurology, London, United Kingdom. ¹²These authors contributed equally: Fernando Bartolome and Agnieszka Krzyzanowska. ✉e-mail: fbartolome.imas12@h12o.es; carroeva@h12o.es

protecting therefore CSF against external toxic insults. Works carried out by Jean Marie Serot *et al.*, found choroid plexus functions of secretion, synthesis, and transport were deteriorated in AD as they observed morphological modifications including epithelial atrophy, fibrosis and calcifications of stroma, and thickened basement membrane¹¹. These impairments resulted in lower turnover and CSF stasis, reduced transthyretin levels, a sequestering protein synthesised by choroid plexus, and oligomerisation and subsequent accumulation of A β (reviewed in¹²). Also, it was demonstrated that A β peptides accumulation in choroid plexus is largely responsible for an increased level of oxidative stress and cell death^{7,13}. A decreased activity of enzymes involved in oxidative phosphorylation¹⁴ and mitochondrial activity⁷, may also contribute to impair protein synthesis in choroid plexus. The observed decrease in the choroid plexus functional activity would be partially correlated with reduced protein secretion and mentioned CSF renewal, which may be involved in the initiation and progression of AD¹². Although the detailed mechanism of A β -induced toxicity in choroid plexus is unclear, perturbation of Ca²⁺ homeostasis, and destabilisation of cellular metabolism by pronounced membrane permeabilisation might likely play an important role.

Annexin A5, a Ca²⁺-regulated, phospholipid-binding protein belongs to the annexins superfamily. This protein is abundantly expressed in a wide range of tissues¹⁵ with intra- and extracellular locations¹⁶. Although annexin A5 is extensively used as an indicator of early apoptosis, it was demonstrated that annexin A5 exerts protective functions including inhibition of proinflammatory response and improvement of cardiac function and survival during endotoxemia in mice¹⁷. Also, annexin A5 was found interacting with amyloidogenic proteins reducing its toxicity in neurodegenerative diseases and type II diabetes mellitus¹⁸. It was also shown annexin A5 provided protection against A β cytotoxicity, and it was proposed that this effect occurs by competitive interaction with phosphatidylserine (PS) on the membrane surface^{19–21}.

Annexins are predominately located within the cell, where they mediate cellular processes such as exocytosis and endocytosis, membrane structure and generation of lipid rafts, but also extracellular roles such as inflammation^{22,23}. Particularly, it was reported annexin A5 has antithrombotic properties, reducing vascular inflammation and improving endothelial function^{24–26}. Annexin A5 was proposed as biomarker in heart injury²⁷ and also in nephrotic syndrome²⁸. Moreover, annexin A5 was associated with various neuropathological conditions. Levels of annexin A5 were reported reduced in CSF from Parkinson's disease (PD) patients²⁹. It was suggested that such reduction resulted as consequence of protein consumption during neuronal apoptosis²⁹. Plasma levels of annexin A5 were found significantly higher in AD patients compared with healthy individuals³⁰. These works suggested a defensive function for annexin A5 in these neurodegenerative diseases based on its interacting role with amyloidogenic proteins, islet amyloid polypeptides and α -synuclein inclusions by reducing the toxicity of these proteins and aggregates¹⁸.

Using a mass proteomic based study, we previously found changes in annexin A5 protein levels in choroid plexus from AD patients³¹. The present study was focused on examining the potential effects of annexin A5 on A β toxicity in choroid plexus. For that purpose, we analysed choroid plexus tissue samples and CSF from MCI and AD patients, and choroid plexus primary cultures. Here, we show annexin A5 levels in CSF were found progressively increased as the disease stage increased in severity. Simultaneously, annexin A5 levels were found decreased with the disease severity in choroid plexus, in opposite way A β burden and cell death. We also show that annexin A5 may play a protective role in A β -induced cell toxicity in choroid plexus by a Ca²⁺-dependent mechanism.

Results

Annexin A5 levels are increased in CSF from AD patients. By doing a mass proteomic based study, we previously found annexin A5 protein levels were differentially expressed in choroid plexus from AD patients compared with healthy controls³¹. Here, we show annexin A5 levels were significantly increased in CSF from MCI and moderate AD patients determined by ELISA (Fig. 1a). We also checked by Western Blot annexin A5 levels in choroid plexus from brain donors with AD pathology and healthy subjects. Annexin A5 protein levels were significantly lower in Braak stages III/IV and V/VI compared with control samples (Fig. 1b). In contrast with our previous work³¹, by increasing the number of samples here we increased the variability losing the significance when comparing AD subjects (stages I–II) with control. When comparing last AD stages with controls, variability was reduced, and results reflect a significant reduction in annexin A5 levels in advanced AD stages compared with aged-matched control subjects. Together, these results could suggest annexin A5 levels in choroid plexus progressively are reduced starting at early AD clinical stages.

A β -related choroid plexus cell death. AD-related pathology was confirmed analysing the A β load in choroid plexus by immunohistochemistry using an anti-A β antibody (Fig. 2a). The progressive pattern of A β accumulation in choroid plexus was estimated using an A β ₄₂ human specific ELISA kit (Fig. 2b). A β ₄₂ burden was significantly higher at Braak stages III/IV and stages V/VI when compared with control cases (Fig. 2b). The effects of A β accumulation determined in choroid plexus using a Cell Death Detection ELISA kit resulted in progressive increased cell death in AD subjects that was significantly higher at Braak stages V/VI compared with healthy donors (Fig. 2c). These results were consistent with the previously reported findings showing deleterious effects of A β in choroid plexus from AD subjects and the AD transgenic APP/PS1 mouse model⁷. It is important to note that the observed progressive A β accumulation and cell death in choroid plexus match with the reduced annexin A5 levels (Fig. 1b), more evident at late AD stages (III–VI) (Fig. 2d).

A β induces Annexin A5 release outside choroid plexus cells. Annexin A5 may be secreted extracellularly and increased annexin A5 levels were previously found in the supernatant of A β ₄₂-treated neuronal cells³². Hence, we asked if changes in annexin A5 levels between choroid plexus and CSF could be related to A β overload in choroid plexus. We used rat primary cultures of epithelial choroid plexus cells treated with oligomerised A β ₄₂ (10 μ M) at 6, 12, 24 and 48 hours. A β exposure in choroid plexus cells resulted in reduced annexin A5 protein

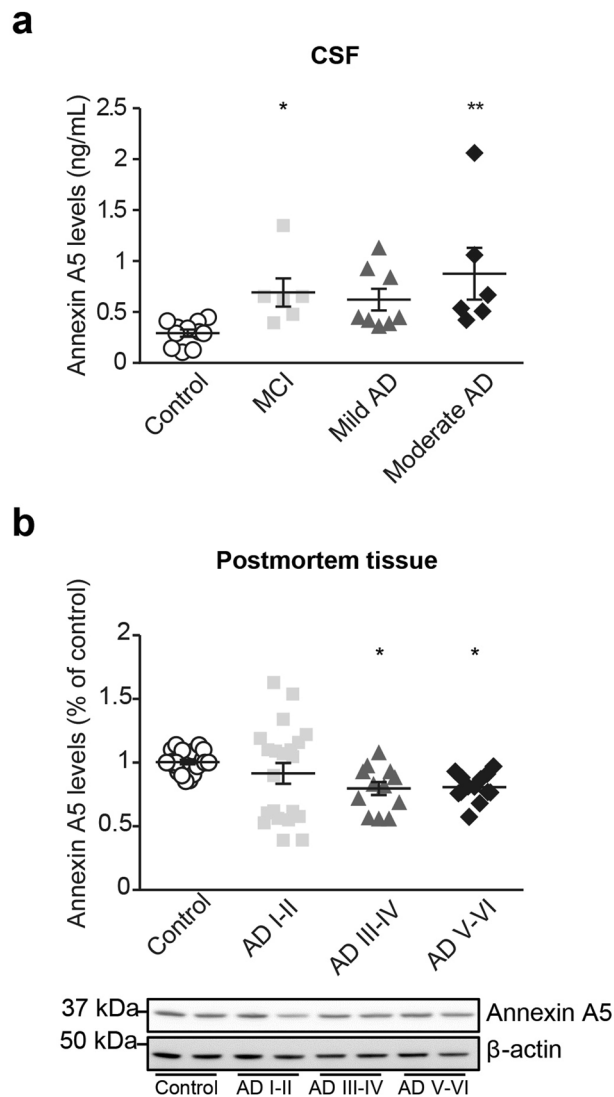


Figure 1. CSF and choroid plexus annexin A5 protein levels were differentially expressed in AD patients. **(a)** Scatter plot showing CSF levels of annexin A5 protein in healthy donors and clinically diagnosed MCI and AD patients determined by ELISA. Annexin A5 levels in CSF samples were found higher in MCI and AD patients compared with controls ($*p < 0.05$, $**p < 0.01$; control $n = 11$; MCI $n = 6$; Mild AD $n = 8$; Moderate AD $n = 6$). In all cases, each individual value is shown along with the mean \pm SEM per group. **(b)** Scatter plot showing annexin A5 protein levels in choroid plexus from AD and healthy donors. Annexin A5 levels were significantly reduced in choroid plexus from Braak stages III/IV and V/VI compared with control samples ($*p < 0.05$; control $n = 22$; AD I-II $n = 21$; AD III-IV $n = 12$; AD V-VI $n = 13$). In all cases, each individual value is shown along with the mean \pm SEM per group. Bottom images show representative western blots. These images were cropped from full-length blots and they are shown in the Supplementary Information section.

levels in a time course-dependent manner (Fig. 3a). This reduction was significant compared with untreated cells 24 and 48 hours after $A\beta$ treatment (Fig. 3a). Conversely, $A\beta$ induced a time course-dependent increase of annexin A5 in the extracellular medium (Fig. 3b). Such annexin A5 increase in supernatant was clearly significant 24 and 48 hours after $A\beta$ treatment (Fig. 3b).

Annexin A5 restores the $A\beta$ -induced impairments on autophagy. A number of studies demonstrate autophagy is disrupted at one point in the progression of AD^{33,34}. This pathway may degrade accumulated aberrant proteins and peptides such as $A\beta$. Results above could suggest that annexin A5 may be beneficial in choroid plexus from AD patients; therefore we investigated the effect of annexin A5 on autophagy. Analysis of autophagy markers in postmortem tissue from AD and healthy donors by immunoblotting, showed significantly increased LC3-II levels in choroid plexus from all AD stages including early AD (Fig. 4a) and significantly increased p62 levels at Braak stages I-IV (Fig. 4b). These results may suggest both, increased autophagy induction and disrupted autophagosome – lysosome fusion^{35,36}. Then we investigated annexin A5 effects on $A\beta$ -disrupted autophagy flux in choroid plexus cultures from rats. Cells were treated with and without annexin A5 for 1 hour and then exposed

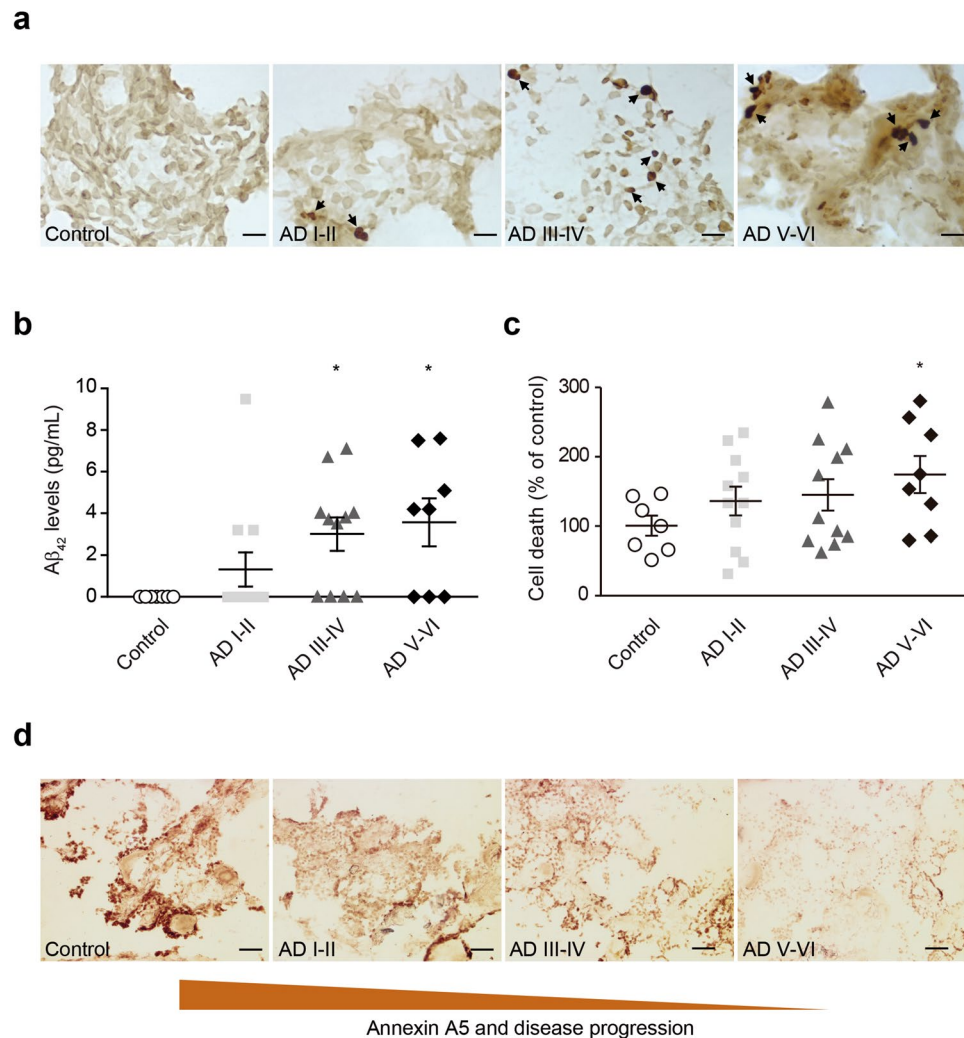


Figure 2. A β deposits and cell death in choroid plexus from AD patients. **(a)** Representative micrographs showing A β deposits in choroid plexus from early and advanced AD cases compared with healthy donors. Scale bar = 20 μ m. **(b)** Quantified levels of A β burden in choroid plexus from healthy donors compared with AD subjects measured by ELISA (Cell Death Detection ELISAPLUS kit, Roche). Scatter plot reveals a progressive increase in A β levels in choroid plexus samples from AD subjects compared with control group ($*p < 0.05$; control $n = 7$; AD I-II $n = 12$; AD III-IV $n = 11$; AD V-VI $n = 8$). In all cases, each individual value is shown along with the mean \pm SEM per group. **(c)** Cell death analysis in choroid plexus from control and AD patients was measured using Cell Death Detection ELISAPLUS kit. Scatter plot shows a significant increase in cell death in choroid plexus from advanced AD patients (Braak stages V–VI) compared with control subjects ($*p < 0.05$; control $n = 7$; AD I-II $n = 11$; AD III-IV $n = 11$; AD V-VI $n = 8$). In all cases, each individual value is shown along with the mean \pm SEM per group. **(d)** Representative micrographs showing annexin A5 immunostaining in choroid plexus from early and advanced AD cases compared with healthy donors. Scale bar = 20 μ m.

to oligomerised A β_{42} to avoid extracellular A β sequestering by annexin A5, thereby preventing the toxicity. Immunoblotting revealed that A β_{42} exposure resulted in significantly elevated LC3-II and p62 levels compared with untreated cells suggesting autophagosome accumulation (Fig. 4c,d, respectively). Annexin A5 treatment in cells restored the LC3-II and p62 levels being similar to the obtained values in untreated or cells treated with annexin A5 only (Fig. 4c,d, respectively). In summary, the above results could indicate annexin A5 abolished the A β -induced impairments on autophagy in choroid plexus cells.

Annexin A5 protects against A β -induced apoptosis. It was previously shown annexin A5 inhibited A β toxicity in neuronal cell cultures^{16,17,19,20,34,37}. We further investigated annexin A5 effect on A β -induced toxicity in choroid plexus cells. As A β -induced autophagy may precede A β -induced toxicity we tested the biological role of annexin A5 on cell viability carrying out bioactivity assays with choroid plexus cell cultures. Cells were previously treated with and without annexin A5 for 1 hour and then exposed to oligomerised A β_{42} (10 μ M) for 48 hours (Fig. 5). A β_{42} induced 25% decrease in cell viability in choroid plexus cultures, as assessed by cell counting kit (CCK) assay, compared with control (Fig. 5a). Annexin A5 completely prevented cell loss when was added prior to A β_{42} (Fig. 5a). The reduction in

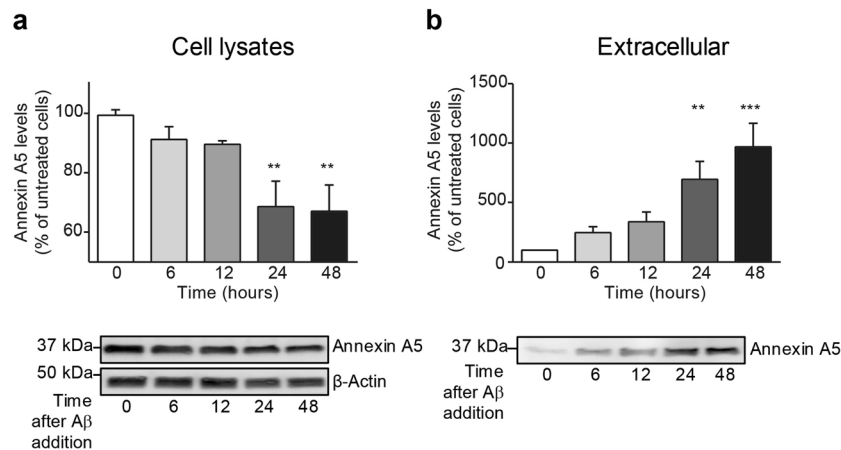


Figure 3. Analysis of intra- and extracellular annexin A5 levels in choroid plexus cultures after A β incubation. **(a)** Annexin A5 levels in epithelial choroid plexus cell cultures incubated with oligomerised A β_{42} for 6, 12, 24 and 48 hours determined by Western blot. Annexin A5 levels are shown as percentage of untreated cells. β -actin was used as loading control. Histogram reveals a progressive decrease in annexin A5 levels in cells incubated with A β_{42} already significant at 24 hours after A β_{42} addition ($**p < 0.01$; $n = 4$). Representative bands of annexin A5 protein levels in choroid plexus cells at 0, 6, 12, 24 and 48 hours after A β_{42} addition (bottom panel). These images were cropped from full-length blots and they are shown in the supplementary information section. In all cases data represents mean \pm SEM. **(b)** Annexin A5 levels in extracellular medium of A β_{42} -incubated choroid plexus cells for 0, 6, 12, 24 and 48 hours. Histogram shows a progressive increase of annexin A5 levels in extracellular medium which is already significant 24 hours after A β_{42} incubation (upper panel) ($**p < 0.01$; $***p < 0.001$; $n = 4$). Representative bands of annexin A5 protein levels in extracellular medium at 0, 6, 12, 24 and 48 hours after A β_{42} addition (bottom panel). This image was cropped from a full-length blot shown in the Supplementary Information section. In all cases data represents mean \pm SEM.

cell viability on choroid plexus cells and the protective role of annexin A5 was studied analysing apoptotic cell death using the LIVE/DEAD Viability/Cytotoxicity Kit (Fig. 5b,c). 48 hours after incubation with A β_{42} (10 μ M), a significant increase of apoptotic cell death in choroid plexus cultures was found (Fig. 5b,c). The presence of annexin A5 attenuated the A β_{42} -induced apoptosis, recovering the amount of living cells and reducing the cell loss (Fig. 5b,c).

Annexin A5 attenuates A β -induced impairments on mitochondrial function and [Ca $^{2+}$] homeostasis in choroid plexus epithelial cells. Both, apoptosis and autophagy are two cellular processes closely linked to mitochondria and mitochondrial health and function is reflected in the $\Delta\Psi_m$. By using the fluorescent indicator TMRM, we analysed the $\Delta\Psi_m$ (Fig. 6a). This dye accumulates in active mitochondria with intact membrane potentials, therefore the more fluorescence, the more mitochondrial health and quality. A significant decrease in $\Delta\Psi_m$ was observed in A β -exposed choroid plexus cells reducing the TMRM signal to $74 \pm 3\%$ compared with either untreated or cells treated with annexin A5 (Fig. 6b). Treatment of A β -exposed choroid plexus cells with annexin A5 prevented the reduction in the $\Delta\Psi_m$ as TMRM signal showed similar values to untreated cells or cells with annexin A5 (Fig. 6b). Mitochondria are master regulators of Ca $^{2+}$ homeostasis³⁸ that simultaneously is linked to autophagy and apoptotic cell death regulation. Because annexin A5 is a Ca $^{2+}$ binding protein we hypothesised that the protective role of annexin A5 could be related to its Ca $^{2+}$ binding capacity. This could be supported by findings in which was demonstrated A β -induced toxicity in neurons involved perturbation of Ca $^{2+}$ homeostasis³⁹. We analysed Ca $^{2+}$ flux upon physiological Ca $^{2+}$ stimuli in choroid plexus cells incubated for 24 hours with oligomerised A β_{42} in absence or presence of annexin A5 (Fig. 6c). Ca $^{2+}$ signal was evaluated using fura-2. Purinergic receptors in epithelial choroid plexus cells were stimulated with ATP allowing the massive release of Ca $^{2+}$ from the endoplasmic reticulum (ER) to the cytosol which was ratiometrically quantified (Fig. 6c, top panels). After recovery, mitochondrial Ca $^{2+}$ uptake was analysed by adding the uncoupler FCCP and the amount of Ca $^{2+}$ was quantified (Fig. 6c, top panels). Upon physiological Ca $^{2+}$ stimuli, changes in $\Delta\Psi_m$ were simultaneously analysed using Rh123 and the fluorescence was also quantified (dequench mode, Fig. 6c, bottom panels). ATP application to A β -treated choroid plexus cells was associated to loss of $\Delta\Psi_m$ as Rh123 signal increased by 23% before FCCP addition. Annexin A5 treatment to A β -incubated choroid plexus cells prevented the mitochondrial depolarisation as Rh123 fluorescence did not increase after ATP addition. We found that A β_{42} incubation resulted in a significantly higher Ca $^{2+}$ release from the ER in response to ATP in choroid plexus cells (Fig. 6d, left panel). Simultaneous incubation with A β and annexin A5 restored the ATP-induced Ca $^{2+}$ release from the ER in choroid plexus cells resulting in a smaller Ca $^{2+}$ signal similar to the obtained in untreated or only annexin A5 treated cells (Fig. 6d, left panel). Mitochondrial Ca $^{2+}$ uptake after FCCP addition was also higher in A β treated cells compared with untreated or only annexin A5 treated cells (Fig. 6d, right panel). Treatment of choroid plexus cells with annexin A5 under A β presence restored the mitochondrial Ca $^{2+}$ uptake reaching similar levels of the untreated cell or cells treated with annexin A5 (Fig. 6d, right panel). Together, these results confirmed

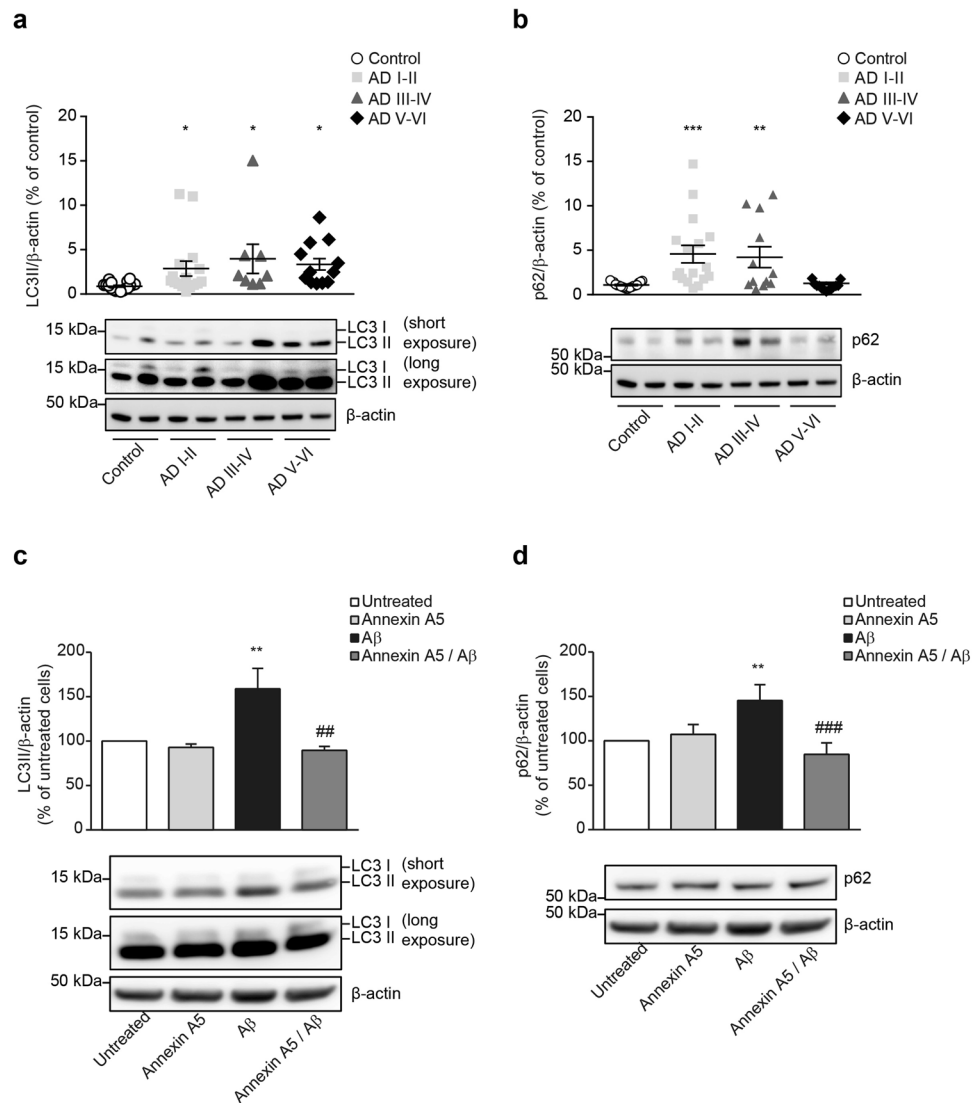


Figure 4. Impaired autophagy in AD choroid plexus. **(a,b)** LC3-II **(A)** and p62 **(b)** protein levels in choroid plexus from healthy donors and AD patients from I, II, III, IV, V and VI Braak stages determined by Western blot. β-actin was used as loading control and data are shown as percentage of untreated cells. **(a)** Scatter plot indicates that autophagic marker LC3-II is significantly increased at early AD stages (Braak I-II). **(b)** p62 is significantly increased at early (Braak I-II) and mid (Braak III-IV) AD stages but decreased at late AD stages (Braak V-VI). Representative Western blot showing LC3-II **(a)** and p62 **(b)** levels in choroid plexus samples from healthy donors, and AD are shown. These images were cropped from full-length blots and they are shown in the Supplementary Information section. (* $p < 0.05$, ** $p < 0.01$, *** $p < 0.001$; control $n = 19$; AD I-II $n = 17$; AD III-IV $n = 12$; AD V-VI $n = 13$). In all cases, each individual value is shown along with the mean \pm SEM per group. **(c,d)** LC3-II **(c)** and p62 **(d)** protein levels in epithelial choroid plexus cell cultures incubated with and without oligomerised A β_{42} (10 μ M) for 24 hours under presence or absence of annexin A5 (15 μ g/ml). β-actin was used as loading control and data are shown as percentage of untreated cells. **(c)** Autophagic marker LC3-II is significantly increased upon A β_{42} incubation compared with untreated or annexin A5-treated cells. Annexin A5 co-incubation restored the A β_{42} -increased autophagic markers levels similar to untreated cells. **(d)** Autophagic marker p62 is significantly increased upon A β_{42} incubation compared with untreated or annexin A5-treated cells. Annexin A5 co-incubation restored the A β_{42} -increased autophagic markers levels similar to untreated cells. Representative Western blot showing LC3II **(c)** and p62 **(d)** levels in epithelial choroid plexus cell cultures are shown. These images were cropped from full-length blots and they are shown in the Supplementary Information section. (** $p < 0.01$ versus untreated cells; ## $p < 0.01$, ### $p < 0.001$ versus A β_{42} -treated cells; $n = 6$). In all cases data represents mean \pm SEM.

annexin A5 exerts its protective role on A β -induced autophagy and apoptotic cell death in choroid plexus in a Ca $^{2+}$ -dependent manner controlled by mitochondria.

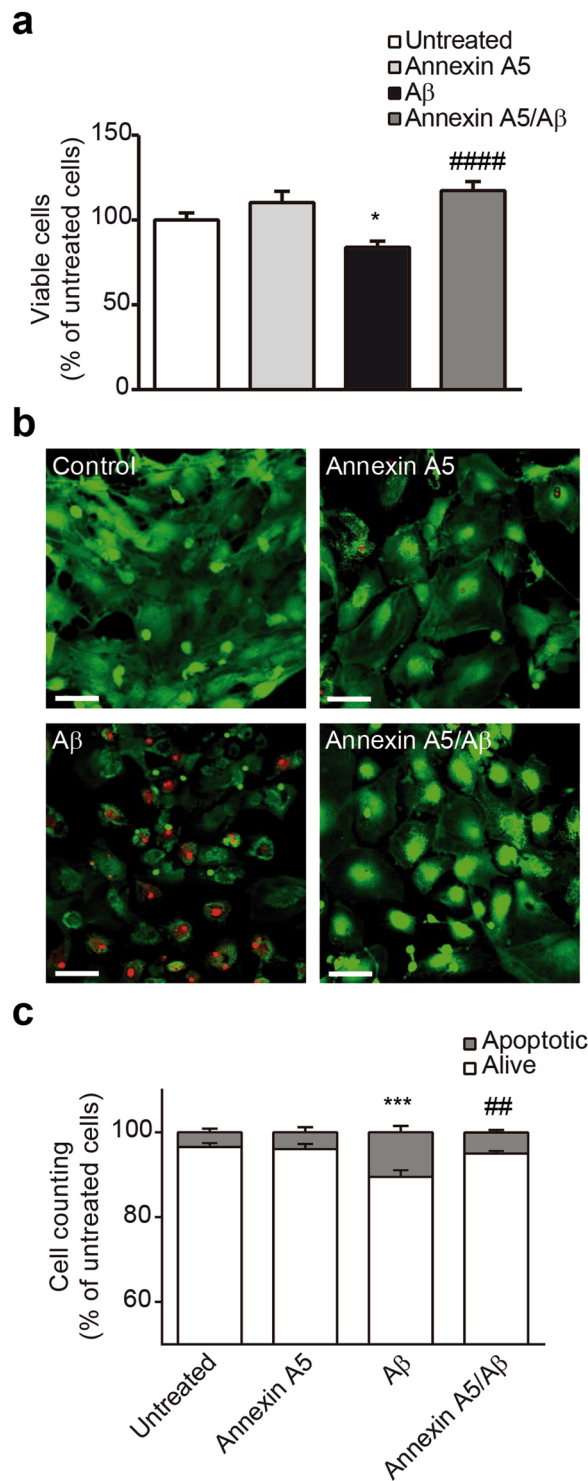


Figure 5. Annexin A5 restores the A β -induced cell viability reduction and apoptosis. **(a)** Epithelial choroid plexus cell viability after incubation with and without oligomerised A β_{42} (10 μ M) for 48 hours in absence or presence of annexin A5. A significant decrease in cellular viability was found in A β_{42} incubated cells compared with untreated cells or cells treated with annexin A5 only. Co-administration of annexin A5 (15 μ l/ml) and A β_{42} (10 μ M) restored cell viability in choroid plexus epithelial cell cultures (* p < 0.05 versus untreated cells; #### p < 0.0001 versus A β_{42} -treated cells; n = 7). In all cases, data represents mean \pm SEM. **(b)** Apoptotic cell death was analysed using the LIVE/DEAD Viability/Cytotoxicity Kit (Molecular Probes). Fluorescent images of epithelial choroid plexus cell culture show living cells (green) and apoptotic cells (red). Cells were incubated with and without oligomerised A β_{42} (10 μ M), in absence and presence of annexin A5 (15 μ l/ml). Scale bar = 44 μ m. **(c)** Counting alive (green) and apoptotic (red) cells shows that A β_{42} incubation induced a significant increase of apoptotic cells compared with untreated or annexin A5 treated cells. Co-administration annexin A5 and A β_{42} reduced the number of apoptotic cells (*** p < 0.001 versus untreated cells; ## p < 0.01 versus A β_{42} -treated cells; n = 4). In all cases, data represents mean \pm SEM.

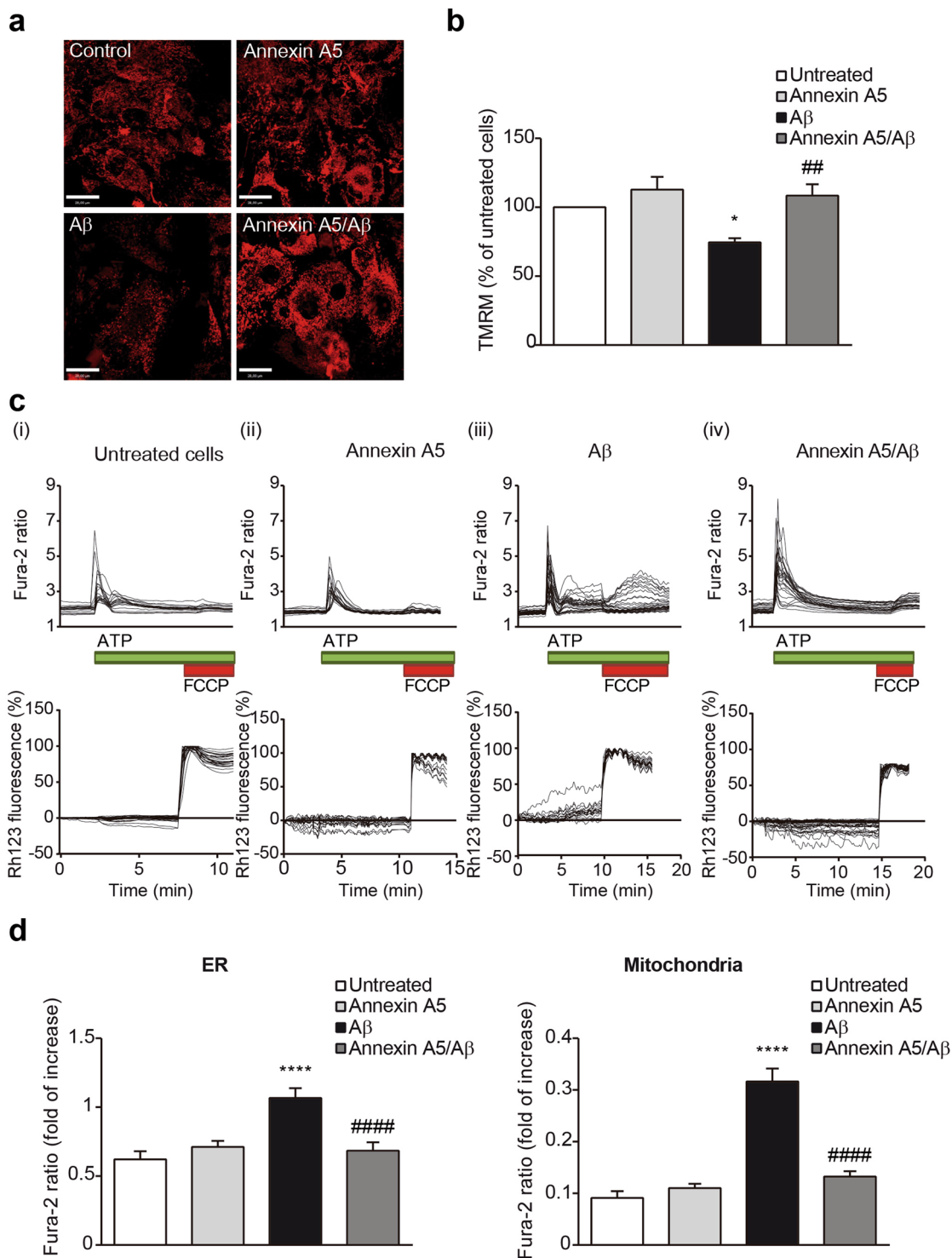


Figure 6. Annexin A5 restores mitochondrial depolarisation in A β -treated choroid plexus cultures in a Ca $^{2+}$ -dependent manner. **(a)** Representative images of tetramethyl-rhodamine methylester (TMRM) fluorescence used in redistribution mode (40 nM) in choroid plexus cultures incubated with and without oligomerised A β_{42} (10 μ M), in absence and presence of annexin A5 (15 μ l/ml). **(b)** Annexin A5 restored the A β -induced mitochondrial depolarisation. Data were normalised to untreated cells and are represented as mean \pm SEM from at least three independent experiments. (* p < 0.05 versus untreated cells; ## p < 0.01 versus A β_{42} -treated cells; n = 4). **(c)** Traces showing changes-over time in fura-2 (upper panels) and simultaneous rhodamine 123 (Rh123) (bottom panels) fluorescence in choroid plexus epithelial cells upon physiological Ca $^{2+}$ stimuli. Physiological Ca $^{2+}$ was induced by addition of ATP (100 μ M). Following Ca $^{2+}$ release from ER, FCCP (1 μ M) was added to obtain the maximal mitochondrial depolarisation allowing mitochondrial Ca $^{2+}$ release. Upon stimulation of choroid plexus cells with ATP, Ca $^{2+}$ stored in the ER was released and profound mitochondrial depolarisation was found in A β -incubated cells as shown by the increase in the Rh123 signal (iii). This effect was

not observed in untreated cells (i) or annexin A5-treated cells only (ii). Annexin A5 treatment prevented the mitochondrial depolarisation when Ca^{2+} stimulus was added (iv). (d) Histograms showing ER Ca^{2+} (left panel) and mitochondrial Ca^{2+} levels (right panel) after addition of ATP and FCCP respectively as explained above. ER Ca^{2+} in choroid plexus cells incubated with $\text{A}\beta$ were higher compared with untreated cells or annexin A5-treated cells only. Annexin A5 co-treatment restored the $\text{A}\beta$ -induced increase of ER Ca^{2+} levels. Mitochondrial Ca^{2+} in $\text{A}\beta$ -incubated choroid plexus cells was significantly higher compared with untreated cells or annexin A5-treated cells only. These levels were restored upon co-incubation with annexin A5. Data were normalised to untreated cells and are represented as mean \pm SEM from at least three independent experiments. (*** $p < 0.0001$ versus untreated cells; **** $p < 0.0001$ versus $\text{A}\beta_{42}$ -treated cells; $n = 4$).

Discussion

Annexins are widely distributed among tissues and their ubiquitous distribution suggests they have important roles in cell biology. In particular, annexin A5 has been found exerting anti-inflammatory, anticoagulant and anti-apoptotic functions^{40–46}. In endothelial cells, annexin A5 was able to protect against vascular inflammation contributing to protect barrier integrity²⁵. Expression of other annexins, annexin A1, A4 and A6, was described in choroid plexus^{47,48}, but little is known about expression and role of annexin A5 in this brain structure. Here we report increased annexin A5 levels in CSF from clinically diagnosed MCI and AD patients and simultaneous reduced annexin A5 levels in choroid plexus from AD brains. These findings are accompanied by increased $\text{A}\beta$ overload in choroid plexus related to the disease severity and significantly altered autophagic flux and increased cell death at late AD stages. *In vitro*, we also demonstrate that annexin A5 extracellular release in choroid plexus cells could be $\text{A}\beta$ -overload dependent. We propose that $\text{A}\beta$ in choroid plexus may induce increased autophagosome accumulation. Such effects result finally in increased cell death and annexin A5 down-regulation. On the other hand, annexin A5 protects against $\text{A}\beta$ toxicity restoring the $\text{A}\beta$ -induced Ca^{2+} homeostasis dysregulation linked to the mitochondrial health and function. Together, our findings suggest that annexin A5 plays a crucial role in maintaining physiological protection of blood-CSF barrier that is impaired in AD.

The higher levels of annexin A5 found in CSF from MCI and AD subjects compared with healthy donors suggests that secreted annexin A5 may indicate early changes in choroid plexus from these patients. Increased annexin A5 levels were also found in plasma from AD patients and the AD transgenic mouse model Tg2576³². We suggest that choroid plexus epithelial cells contribute to increase the annexin A5 levels in CSF along with other sources as neurons. Our results indicate CSF levels of annexin A5 become increased even at early stages of disease, including MCI, when $\text{A}\beta$ accumulation in the brain becomes evident. This is consistent with other findings observed in neuronal cell cultures, describing increased annexin A5 levels in the supernatant of $\text{A}\beta_{42}$ -treated cells³².

$\text{A}\beta$ deposition in brains of AD patients agrees with the hypothesis suggesting $\text{A}\beta$ accumulation as the main cause for neuronal cell death^{1,5,49}. Exposure of cells to $\text{A}\beta$ peptides cause typical apoptotic cell death^{50,51}, although lower $\text{A}\beta$ concentrations appear to only affect expression of neuronal apoptotic genes, without directly causing apoptosis^{52,53}. Here we show that $\text{A}\beta$ accumulation in AD is also present in choroid plexus. This observation was found gradually increasing as the disease progresses and is consistent with the increased cell death observed in choroid plexus from AD subjects. We demonstrate $\text{A}\beta$ overload in choroid plexus cultures induced annexin A5 reduction in cells and subsequently increased annexin A5 in extracellular medium. Annexin A5 release outside cells occurs from the cellular apical compartment as has been demonstrated in epithelial cell cultures^{46,54}. Upon Ca^{2+} stimulation, cytoplasmic annexin A5 is translocated to the plasma membrane while nuclear annexin A5 is moved to the nuclear membrane, in all cases binding to phosphatidylserine (PS)⁵⁵. As $\text{A}\beta$ also binds PS, both annexin A5 and $\text{A}\beta$ could exert competitive interaction to each other. Reduced levels of intracellular annexin A5 result in lower competitive inhibition with $\text{A}\beta$ at PS interaction site leading to increasing $\text{A}\beta$ -induced cytotoxicity¹⁹. We may suggest $\text{A}\beta$ overload in patient choroid plexus could induce annexin A5 drain from these cells, hence contributing to the observed increased levels in CSF.

Our experiments show that annexin A5 restores the $\text{A}\beta$ -induced autophagic flux impairments in choroid plexus cells reducing the $\text{A}\beta$ -increased levels of LC3-II and p62. Previous works showed elevated LC3-II and p62 levels in brains from AD patients at different stages of disease^{56,57}. Here we found an increase in these autophagy markers in human choroid plexus suggesting that such increase is due to $\text{A}\beta$ overload. In support of this observation several works showed similar effects increasing autophagy markers after $\text{A}\beta$ incubation in human neuroblastoma H4 cells⁵⁸ and in cells overexpressing mutant forms of *PSEN2* and *APP*, both linked to $\text{A}\beta$ overproduction in AD familial cases^{59,60}. Therefore, we may suggest an induction of autophagy is triggered in choroid plexus due to $\text{A}\beta$ overload. Then autophagosomes containing $\text{A}\beta$ cannot be fused with lysosomes resulting in their accumulation and subsequent increased levels of autophagic markers LC3-II and p62. Apart of the mentioned cellular models^{59,60} this dual effect has been also observed in AD brains showing high autophagy flux. Such increased flux would try to maintain low $\text{A}\beta$ levels through autophagic clearance but this is followed by impaired autolysosomal proteolysis^{33,34,57,61–63}. We found that annexin A5 treatment restored the levels of autophagy markers to similar values that those obtained in untreated cells. We suggest the annexin A5 effect on autophagy may work enhancing autophagosome – lysosomes fusion allowing lysosomal cargo degradation. This agrees with other observations where annexin A5 was proposed stimulating autophagy⁶⁴. In this work, authors showed that overexpression of annexin A5 in HEK293T cells decreased LC3-II levels. They proposed such decrease was produced by the annexin A5 effect of increasing the autophagosome conversion into autolysosomes and enhancing lysosomal proteolysis⁶⁴.

Linked to the protective role on autophagy could be the observation that annexin A5 reduced the number of $\text{A}\beta$ -induced apoptotic cells. The idea of $\text{A}\beta$ -induced cell death is preceded by impaired autophagy was also showed by other authors^{65,66}. Further analysis about this connection was discussed by Nixon and Yang where they

	Control	MCI	Mild AD	Mod AD	p-value
	(n = 26)	(n = 26)	(n = 20)	(n = 20)	
Age, mean (SD)	70.9 (9.2)	70.7 (7.3)	76.6 (6.5)	78.3 (3.6)	0.01
Sex female, n (%)	14 (53.8%)	15 (57.7%)	11 (55.0%)	10 (50.0%)	ns
MMSE, mean (SD)	29.0 (1.2)	24.5 (3.4)	19.3 (4.4)	12.3 (5.2)	<0.001
CDR	0	0.5	1	2.3	<0.001
ApoE ϵ 4, %	0%	41.6%	46.1%	40.2%	0.01
CSF A β ₄₂ , mean (sem)	885.2 (105.2)	457.3 (53.0)***	513.8 (95.9)**	339.1 (46.2)***	<0.001
CSF t-tau, mean (sem)	394.5 (54.6)	534.8 (123.5)	690.4 (73.4)*	982.8 (105.4)**	0.01

Table 1. Demographic and clinical characteristics of CSF donors. MCI: mild cognitive impairment; AD: Alzheimer's disease; Mod: moderate-severe; SD: standard deviation; MMSE: Minimal Status Examination; ns: non-significant. # p-value indicates statistical differences between all groups; *p < 0.05, **p < 0.01, ***p < 0.001, versus control group.

proposed defects in autophagy promoting apoptotic cell death in neurodegenerative diseases⁶⁷. This is consistent with our results as we observed a reduction in autophagy markers and apoptotic cell death when rat primary cultures of epithelial choroid plexus cells were incubated with A β in presence of annexin A5. Both, stimulation of autophagy and apoptotic cell death are tightly regulated by intracellular Ca²⁺ levels^{68,69}. On this regard, mitochondria play an important role in cells as they control bioenergetics, Ca²⁺ homeostasis and apoptotic cell death. Failures in this regulation have been recognised in neurodegenerative disorders. Here, we show that annexin A5 restored the A β -induced mitochondrial depolarisation reflected by a reduction in the mitochondrial membrane potential which mirrors the mitochondrial health and function. Therefore, mitochondrial depolarisation may indicate altered Ca²⁺ homeostasis regulation. Indeed, our work show A β impaired Ca²⁺ homeostasis, and annexin A5 prevented this effects. A β exposure made the choroid plexus cells to increase the ER Ca²⁺ stores. Then, by inducing Ca²⁺ signal, mitochondrial Ca²⁺ uptake was higher. Both effects were restored by annexin A5 incubation. It has been shown A β affects intracellular Ca²⁺ concentration by generating Ca²⁺ permeable channels in plasma membrane of neurons and astrocytes^{70,71}. Works carried out in neuronal cells showed A β exposure induced Ca²⁺ homeostasis impairments⁷²⁻⁷⁵. *In vivo*, elevated Ca²⁺ levels in neuronal cytoplasm were linked to A β ₄₂ accumulation⁷⁶. The observed protective role of annexin A5 in the A β -induced autophagy impairments and cell death could be related to its affinity binding preferentially acidic phospholipids in a Ca²⁺ dependent manner²². This could be in line with the observed annexin A5 ability to interact with membrane PS. Through this interaction, it was found that annexin A5 protected neuronal cells against A β toxicity by competitive inhibition as both, A β oligomers and annexin A5 showed binding affinity to PS in the cell membrane in a Ca²⁺-dependent manner^{19,20}. In a different scenario, we may also explain the protective role of annexin A5 on A β -induced toxicity by its Ca²⁺ chelating capacity decreasing the intracellular Ca²⁺ concentration. All these observations are consistent with our findings in which we found annexin A5 could have a potential beneficial effect on choroid plexus and such effect is lost in AD along with progressive increased A β accumulation. This beneficial effect of annexin A5 has been proved in other neurodegenerative disorders showing its interaction ability with amyloidogenic proteins¹⁸.

In summary, we show that levels of annexin A5 in choroid plexus from AD are reduced in late stages of disease, accompanied by high A β levels and cell death and simultaneous increased levels of annexin A5 in CSF. The data presented here indicate that annexin A5 protects choroid plexus cells from A β -induced autophagic impairments and apoptosis by a Ca²⁺-dependent mechanism under mitochondrial control.

Material and Methods

All methods were performed following the relevant guidelines and regulations approved by the local ethical review committee from the Hospital 12 de Octubre Research Institute. Other review committees partially involved in the present project were the following: 12 de Octubre Hospital, (Madrid, Spain) and Hospital de la Santa Creu i Sant Pau (Barcelona, Spain) review committees for research related to CSF samples; The Institute of Neuropathology Brain Bank IDIBELL-Hospital Universitari de Bellvitge (Hospitalet de Llobregat, Spain) review committee, The Netherlands Brain Bank (NBB) (Amsterdam, The Netherlands) review committee and Banco de Tejidos, Fundación CIEN (Centro de Investigación de Enfermedades Neurológicas, Madrid, Spain) review committee for research involving the use of choroid plexus samples from human donors. Informed consent was obtained from all participants and/or their legal guardians.

CSF collection. CSF samples (10 ml per subject) from 26 mild cognitive impairment (MCI), 20 mild AD, 20 moderate AD, and 26 healthy control subjects were collected by lumbar puncture upon informed patient consent. All samples were centrifuged at 3000 rpm at 4°C for 10 min to remove any cell and debris, aliquoted in small volumes and stored in low bind polypropylene tubes at -80°C. Samples were obtained from the Hospital 12 de Octubre Neurology Service (Madrid, Spain), and Hospital de la Santa Creu i Sant Pau Neurology Service (Barcelona, Spain). Subjects were clinically diagnosed as probably having AD according to the National Institute on Aging and Alzheimer's Association (NIA-AA) guidelines⁷⁷. MCI was diagnosed in patients with cognitive impairment that did not fulfil the criteria for dementia^{78,79}. All subjects had mini-mental state examination (MMSE) scores available. Inclusion criteria for cognitively normal older individual subjects were MMSE scores 24-30, no history or clinical signs of neurological or psychiatric disease or cognitive symptoms⁸⁰. Subjects'

	Control (n = 22)	AD I-II (n = 21)	AD III-IV (n = 14)	AD V-VI (n = 13)	p-value
Age, mean (SD)	71.2 (10.0)	69.4 (9.9)	78.9 (7.7)	78.3 (6.6)	<0.001
Sex female, n (%)	9 (40.9%)	7 (33.3%)	6 (42.9%)	6 (46.2%)	ns

Table 2. Demographic and clinical characteristics of choroid plexus donors. AD I-VI: Alzheimer disease-related changes, stages of Braak and Braak; SD: standard deviation; ns: non-significant.

consent was obtained according to [Declaration of Helsinki](#), and approval came from the research ethics committee of each responsible institution. Written informed consent was given from all participants or representatives. Subject demographic and clinical characteristics are listed in Table 1.

Tissue samples. Post-mortem choroid plexus tissue was obtained from brain donors diagnosed with AD and control individuals. Frozen samples were supplied by the Institute of Neuropathology Brain Bank IDIBELL-Hospital Universitari de Bellvitge (Hospitalet de Llobregat, Spain), The Netherlands Brain Bank (NBB) (Amsterdam, The Netherlands), and Banco de Tejidos, Fundación CIEN (Centro de Investigación de Enfermedades Neurológicas, Madrid, Spain). In all cases, post-mortem delays before sampling was between 3–8 hours. Subjects' consent was obtained according to the [Declaration of Helsinki](#), and approval came from the research ethics committee of each responsible institution. For all cases, written informed consent is available. Subjects were selected on the basis of post-mortem diagnosis of AD according to neurofibrillary pathology and A β plaques. Control cases were considered those without neurological symptoms and lesions in the neuropathological examination. A total of 70 samples were categorised into four groups, as presented in Table 2.

Choroid plexus cultures. Choroid plexus epithelial cell cultures were prepared as described previously⁸¹. Choroid plexus were dissected from 3–5-day-old Wistar rats (Charles River, MA, USA). ARRIVA guidelines for the care and use of animals were followed. Once disaggregated, choroid plexus epithelial cells were seeded at a 4×10^4 cells/cm² density on laminin-coated plates and maintained in Dulbecco's modified Eagle's medium (DMEM, Thermo Fisher Scientific, MA, USA) supplemented with 10% (v/v) fetal bovine serum (FBS; Thermo Fisher Scientific, MA, USA), 2 mM L-glutamine and 1% penicillin/streptomycin (Thermo Fisher Scientific, MA, USA) at 37°C and 5% CO₂. After 5–7 days on culture cells reached confluence and they were serum-deprived for 2 hours and oligomerised A β_{42} (10 μ M; AnaSpec, Inc., San Jose, CA) was added. In the experiments with annexin A5 (15 μ l/ml; Sigma-Aldrich, St. Louis, USA), this drug was added 1 hour before oligomerised A β_{42} , to allow annexin A5 enter into the cells and avoiding extracellular sequestering of oligomerised A β_{42} . A β_{42} stock was previously dissolved in acetic acid 0.1 M. Oligomeric A β_{42} was prepared by incubating a volume of stock solution in DMEM at 4°C for 24 hours prior addition to the cell cultures as previously described⁸².

Immunohistochemistry. Human choroid plexus tissue was fixed for 24 hours in 4% paraformaldehyde (PFA) by immersion. Then, choroid plexus samples were OCT embedded and stored at –80°C for subsequent cryostat sectioning (Leica, Wetzlar, Germany). 20 μ m thick sections were processed free-floating for immunohistochemistry. To carry out immunohistochemistry for A β deposits, brain slices were 20 min pre-incubated with 88% formic acid and immunolabeled with mouse anti-A β antibody (1:500, MBL, Nagoya, Japan). After overnight incubation, primary antibody staining was revealed using the avidin-biotin complex method (VECTASTAIN Elite ABC Kit, Vector Laboratories, Burlingame, CA) and 3,3'-diaminobenzidine chromogenic reaction (Vector Laboratories, Inc). Images were captured using a light microscope (Zeiss microscope; Carl Zeiss Microimaging, GmbH, Oberkochen, Germany).

ELISA. Levels of human endogenous A β_{42} in choroid plexus fractions from human subjects were determined with human specific ELISA kit (Innotest β -amyloid_{1–42}, Innogenetics, Ghent, Belgium), according to the manufacturer's instructions. Prior to tissue homogenisation, endothelial vessels were removed in order to have pure choroid plexus epithelium. Obtained data were normalised to protein content.

DNA fragmentation undergoing apoptosis was detected in choroid plexus tissue from human subjects with a Cell Death Detection ELISAPLUS kit (Roche, Basel, Switzerland). According to the manufacturer's instructions, unfixed frozen tissue was incubated with incubation buffer (lysis buffer provided in the kit) and tissue lysates were transferred to a streptavidin-coated 96 well microplate and allowing nucleosomes to interact with monoclonal antibodies: antihistone (biotin-labeled) and anti-DNA (peroxidase-conjugated). Finally, the amount of coloured product was determined using a microplate reader.

Annexin A5 levels in CSF from human subjects were determined with specific human ELISA kit (Abcam, Cambridge, UK). Briefly, CSF samples were added to the pre-coated wells, followed by the antibody mix. Finally, the signal intensity was measured at 450 nm using a microplate reader.

Western blot. Conditional medium from choroid plexus cultures was collected and protease and phosphatase inhibitor cocktails (Roche, Basel, Switzerland) were added. Choroid plexus tissue and cultured choroid plexus epithelial cells were homogenised in lysis buffer (50 mM Tris/HCl buffer, pH 7.4 containing 2 mM EDTA, 0.2% Nonidet P-40, 1 mM PMSE, protease and phosphatase inhibitor cocktails – Roche, Basel, Switzerland), and centrifuged for 10 min at 14000 rpm. The supernatant was recovered and stored at –80°C. Protein content from cell lysates, and extracellular medium was determined with the BCA method (Thermo Fisher Scientific, MA, USA). Equal amount of protein (20 μ g per lane) were separated by SDS-PAGE (4–12%) and transferred onto

polyvinylidene difluoride (PVDF) membranes (Millipore, MA, USA). For human choroid plexus tissue homogenates 25 µg of protein were loaded. Non-specific bindings were blocked by incubation in 5% non-fat milk in Tris-buffered saline (100 mM NaCl, 10 mM Tris, pH 7.4) containing 0.1% Tween (TTBS) for 1 hour at room temperature. Afterwards, membranes were 4 °C incubated overnight with mouse anti-annexin A5 antibody (ab54775, 1:1000; Abcam, Cambridge, UK), rabbit monoclonal anti-p62 antibody (ab91526, 1:20000; Abcam, Cambridge, UK), and rabbit polyclonal anti-LC3 antibody (NB100–2220, 1:1000; Novus, CO, USA). Protein loading was monitored using a mouse monoclonal antibody against β-actin (A1978, 1:10000; Sigma-Aldrich, St. Louis, USA). Membranes were then incubated for 1 hour in the appropriate horseradish peroxidase-conjugated secondary antibodies (1:2000; Dako, CA, USA), and immunocomplexes were revealed by an enhanced chemiluminescence reagent (ECL Clarity; Bio Rad, CA, USA). Densitometric quantification was carried out with Image Studio Lite 5.0 software (Li-COR Biosciences, NE, USA). Protein bands were normalised to β-actin levels and expressed as percentage of the control group.

Bioactivity and cell death quantification. *In vitro*, cell viability was assessed using Cell Counting Kit-8 (CCK-8 assay, Sigma, St. Louis, USA) according manufacturer's instructions. Briefly, primary cultures of choroid plexus epithelial cells were incubated 48 hours with and without oligomerised Aβ₄₂ (10 µM) and treated with or without annexin A5 (15 µl/ml). Then, CCK-8 solution was added, and absorbance was measured 1 hour later at 450 nm using a microplate reader.

Cell death was assessed 48 hours after incubation with and without both, oligomerised Aβ₄₂ (10 µM) and annexin A5 (15 µl/ml) using the LIVE/DEAD Viability/Cytotoxicity Kit (Molecular Probes, Thermo Fisher Scientific, MA, USA). Fixed cells were labelled with propidium iodide. Healthy cells were recognised by their morphology and green staining, whereas propidium iodide-positive red cells (with condensed chromatin) were scored as apoptotic. Resulting images were taken using a fluorescence microscopy (Zeiss microscope; Carl Zeiss Microimaging, GmbH, Oberkochen, Germany) at a magnification of 40×. Fluorescence was quantified using the Volocity software (PerkinElmer, Waltham, MA, USA).

Measurement of mitochondrial membrane potential ($\Delta\Psi_m$). $\Delta\Psi_m$ was measured as was described previously⁸³. Briefly, cells plated on 25 mm laminin-coated coverslips and loaded with 40 nM tetramethyl-rhodamine methyl ester (TMRM) in a HEPES-buffered salt solution (HBSS) (composed of 156 mM NaCl, 3 mM KCl, 2 mM MgSO₄, 1.25 mM KH₂PO₄, 2 mM CaCl₂, 10 mM glucose and 10 mM HEPES; pH adjusted to 7.35 with NaOH) for 40 min at room temperature and keeping the dye present in the chamber at the time of recording. TMRM is a cell-permeant fluorescent dye used in the redistribution mode to assess $\Delta\Psi_m$, and therefore, a reduction in TMRM fluorescence represents mitochondrial depolarisation. Confocal images were obtained using a Zeiss 510 microscope equipped with META detection system (Zeiss, Oberkochen, Germany) and × 40 oil immersion objective. Excitation wavelength for TMRM was 560 nm and emission was detected above 580 nm. Z-stack images were obtained and analysed using the Volocity software (PerkinElmer, Waltham, MA, USA) and TMRM values for untreated cells were set to 100%. TMRM values for Aβ₄₂ and/or annexin A5 treated cells were expressed relative to untreated cells.

Imaging of [Ca²⁺]_c. For cytosolic [Ca²⁺]_c ([Ca²⁺]_c) measurements cells were plated on 25 mm laminin-coated coverslips and maintained in DMEM supplemented with 10% (v/v) FBS, 2 mM L-glutamine and 1% penicillin/streptomycin at 37 °C and 5% CO₂. After 5–7 days on culture, media was replaced with HBSS (156 mM NaCl, 3 mM KCl, 2 mM MgSO₄, 1.25 mM KH₂PO₄, 2 mM CaCl₂, 10 mM glucose and 10 mM HEPES, pH adjusted to 7.35) and cells were loaded with fura-2 AM (5 µM; Molecular Probes, Thermo Fisher Scientific, MA, USA) and 0.005% pluronic for 30 minutes. For simultaneous measurement of [Ca²⁺]_c and $\Delta\Psi_m$, rhodamine123 (Rh123, 10 µM; Molecular Probes, Thermo Fisher Scientific, MA, USA) was added into the cultures during the last 15 min of the fura-2 loading period, and cells were then washed. We stimulated P2Y receptors from choroid plexus cells with 100 µM ATP and we added 1 µM carbonyl cyanide-4-(trifluoromethoxy) phenylhydrazone (FCCP) to depolarise mitochondria. Fluorescence measurements were obtained on an epifluorescence inverted microscope equipped with a × 20 fluorite objective. Simultaneous [Ca²⁺]_c and $\Delta\Psi_m$ were monitored in single cells using excitation light provided by a Xenon arc lamp, the beam passing sequentially through 10 nm band pass filters centred at 340, 380 and 490 nm housed in computer-controlled filter wheel (Cairn Research, Kent, UK). Emitted fluorescence light was reflected through a 515 nm long-pass filter to a cooled CCD camera (Retiga, QImaging, Canada). All imaging data were collected and analysed using the Andor software (Belfast, UK). The fura-2 data were not calibrated in terms of [Ca²⁺]_c because of the uncertainty arising from the use of different calibration techniques. The fluorescent signal is quenched by Rh123 accumulation in polarised mitochondria; in response to depolarisation the fluorescence signal is dequenched; an increase in Rh123 signal therefore indicates mitochondrial depolarisation. We normalised the signals between resting level (set to 0) and a maximal signal generated in response to the uncoupler FCCP (1 µM; set to 100%).

Data and statistical analysis. *In vivo* and *in vitro* results are shown related to healthy donors and untreated cells, respectively. All of them are expressed as mean ± standard error of the mean (SEM) in percentage. *In vitro* data were generated from a minimum of three independent replicates per experiment (n = 3) performed in different days. For *in vivo* imaging, each replicate consisted of at least 1 coverslip per condition where a number of 15–30 cells per coverslip were analysed. Statistical analysis and exponential curve fitting were performed using GraphPad Prism 6.01 (GraphPad Software, La Jolla, CA, USA) software. Grubbs outlier filter was used for all data. Statistical significance for multiple comparisons was calculated by one-way ANOVA followed by Fisher's LSD correction. In all cases, statistical significance was set at $p < 0.05$ (* $p < 0.05$, ** $p < 0.01$, *** $p < 0.001$; # $p < 0.05$, ## $p < 0.01$, ### $p < 0.001$, #### $p < 0.0001$).

Ethical approval and informed consent. All participants gave written informed consent for participation. ARRIVA guidelines for the care and use of animals were followed. The project in full was approved by the 12 de Octubre Research Institute ethical review committee. Additionally, research related to CSF samples was also approved by the 12 de Octubre Hospital, (Madrid, Spain) and Hospital de la Santa Creu i Sant Pau (Barcelona, Spain) review committees; research involving the use of choroid plexus samples from human donors was also approved by the Institute of Neuropathology Brain Bank IDIBELL-Hospital Universitari de Bellvitge (Hospitalet de Llobregat, Spain) review committee, The Netherlands Brain Bank (NBB) (Amsterdam, The Netherlands) review committee and Banco de Tejidos, Fundación CIEN (Centro de Investigación de Enfermedades Neurológicas, Madrid, Spain) review committee.

Data availability

The datasets generated and/or analysed during the current study are available from the corresponding author on reasonable request.

Received: 10 February 2020; Accepted: 9 May 2020;

Published online: 10 June 2020

References

- Hardy, J. & Selkoe, D. J. The amyloid hypothesis of Alzheimer's disease: progress and problems on the road to therapeutics. *Science* **297**, 353–356 (2002).
- Goedert, M. & Spillantini, M. G. A century of Alzheimer's disease. *Science* **314**, 777–781 (2006).
- Zheng, H. & Koo, E. H. Biology and pathophysiology of the amyloid precursor protein. *Mol. neurodegeneration* **6**, 27 (2011).
- Koffie, R. M., Hyman, B. T. & Spires-Jones, T. L. Alzheimer's disease: synapses gone cold. *Mol. neurodegeneration* **6**, 63 (2011).
- Selkoe, D. J. Toward a comprehensive theory for Alzheimer's disease. Hypothesis: Alzheimer's disease is caused by the cerebral accumulation and cytotoxicity of amyloid beta-protein. *Ann. N. Y. Acad. Sci.* **924**, 17–25 (2000).
- Dietrich, M. O. *et al.* Megalin mediates the transport of leptin across the blood-CSF barrier. *Neurobiol. Aging* **29**, 902–912, <https://doi.org/10.1016/j.neurobiolaging.2007.01.008> (2008).
- Vargas, T. *et al.* Abeta accumulation in choroid plexus is associated with mitochondrial-induced apoptosis. *Neurobiol. Aging* **31**, 1569–1581 (2010).
- Crossgrove, J. S., Smith, E. L. & Zheng, W. Macromolecules involved in production and metabolism of beta-amyloid at the brain barriers. *Brain Res.* **1138**, 187–195, <https://doi.org/10.1016/j.brainres.2006.12.022> (2007).
- Kalaria, R. N., Premkumar, D. R., Pax, A. B., Cohen, D. L. & Lieberburg, I. Production and increased detection of amyloid beta protein and amyloidogenic fragments in brain microvessels, meningeal vessels and choroid plexus in Alzheimer's disease. *Brain Res. Mol. Brain Res* **35**, 58–68, [https://doi.org/10.1016/0169-328x\(95\)00180-z](https://doi.org/10.1016/0169-328x(95)00180-z) (1996).
- Liu, F. *et al.* gamma-secretase binding sites in aged and Alzheimer's disease human cerebrum: the choroid plexus as a putative origin of CSF Abeta. *Eur. J. Neurosci.* **37**, 1714–1725, <https://doi.org/10.1111/ejn.12159> (2013).
- Serot, J. M., Bene, M. C., Foliguet, B. & Faure, G. C. Morphological alterations of the choroid plexus in late-onset Alzheimer's disease. *Acta neuropathologica* **99**, 105–108 (2000).
- Serot, J. M., Zmudka, J. & Jouanny, P. A possible role for CSF turnover and choroid plexus in the pathogenesis of late onset Alzheimer's disease. *J. Alzheimer's disease: JAD.* **30**, 17–26, <https://doi.org/10.3233/jad-2012-111964> (2012).
- Perez-Gracia, E., Blanco, R., Carmona, M., Carro, E. & Ferrer, I. Oxidative stress damage and oxidative stress responses in the choroid plexus in Alzheimer's disease. *Acta neuropathologica* **118**, 497–504 (2009).
- Preston, J. E. Ageing choroid plexus-cerebrospinal fluid system. *Microsc. Res. Tech.* **52**, 31–37 (2001).
- Rescher, U. & Gerke, V. Annexins—unique membrane binding proteins with diverse functions. *J. Cell Sci.* **117**, 2631–2639, <https://doi.org/10.1242/jcs.01245> (2004).
- Romisch, J. *et al.* Annexins I to VI: quantitative determination in different human cell types and in plasma after myocardial infarction. *Blood Coagul. Fibrinolysis* **3**, 11–17 (1992).
- Arnold, P. *et al.* Recombinant human annexin A5 inhibits proinflammatory response and improves cardiac function and survival in mice with endotoxemia. *Crit. care Med.* **42**, e32–41, <https://doi.org/10.1097/CCM.0b013e3182a63e01> (2014).
- Bedrood, S. *et al.* Annexin A5 directly interacts with amyloidogenic proteins and reduces their toxicity. *Biochemistry* **48**, 10568–10576, <https://doi.org/10.1021/bi900608m> (2009).
- Lee, G., Pollard, H. B. & Arispe, N. Annexin 5 and apolipoprotein E2 protect against Alzheimer's amyloid-beta-peptide cytotoxicity by competitive inhibition at a common phosphatidylserine interaction site. *Peptides* **23**, 1249–1263 (2002).
- Hung, L. W. *et al.* Amyloid-beta peptide (Abeta) neurotoxicity is modulated by the rate of peptide aggregation: Abeta dimers and trimers correlate with neurotoxicity. *J. neuroscience: Off. J. Soc. Neurosci.* **28**, 11950–11958 (2008).
- Ciccotosto, G. D. *et al.* Stereospecific interactions are necessary for Alzheimer disease amyloid-beta toxicity. *Neurobiol. Aging* **32**, 235–248 (2011).
- Gerke, V., Creutz, C. E. & Moss, S. E. Annexins: linking Ca²⁺ signalling to membrane dynamics. *Nat. reviews. Mol. Cell Biol.* **6**, 449–461 (2005).
- Creutz, C. E., Hira, J. K., Gee, V. E. & Eaton, J. M. Protection of the membrane permeability barrier by annexins. *Biochemistry* **51**, 9966–9983, <https://doi.org/10.1021/bi3013559> (2012).
- Domeij, H. *et al.* Annexin A5 inhibits atherogenic and pro-inflammatory effects of lysophosphatidylcholine. *Prostaglandins Other Lipid Mediat* (2013).
- Ewing, M. M. *et al.* Annexin A5 therapy attenuates vascular inflammation and remodeling and improves endothelial function in mice. *Arterioscler. Thromb. Vasc. Biol.* **31**, 95–101 (2011).
- Gu, C., Liu, M., Zhao, T., Zhai, L. & Wang, Y. Recombinant Human Annexin A5 Can Repair the Disrupted Cardiomyocyte Adherens Junctions in Endotoxemia. *Shock* **44**, 83–89, <https://doi.org/10.1097/SHK.0000000000000370> (2015).
- Hofstra, L. & Heymans, S. Annexin A5 and the failing heart; lost or found in translation? *Eur. Heart J.* **28**, 2695–2696, <https://doi.org/10.1093/eurheartj/ehm452> (2007).
- Simsek, B. *et al.* Urinary annexin V in children with nephrotic syndrome: a new prognostic marker? *Pediatr. Nephrol.* **23**, 79–82, <https://doi.org/10.1007/s00467-007-0606-z> (2008).
- Vermes, I., Steur, E. N., Reutelingsperger, C. & Haanen, C. Decreased concentration of annexin V in parkinsonian cerebrospinal fluid: speculation on the underlying cause. *Mov. disorders: Off. J. Mov. Disord. Soc.* **14**, 1008–1010 (1999).
- Sohma, H. *et al.* Evaluation of annexin A5 as a biomarker for Alzheimer's disease and dementia with lewy bodies. *Front. aging Neurosci.* **5**, 15 (2013).
- Krzyzanowska, A. *et al.* Expression of regulatory proteins in choroid plexus changes in early stages of Alzheimer disease. *J. neuropathology Exp. Neurol.* **74**, 359–369, <https://doi.org/10.1097/nen.0000000000000181> (2015).

32. Yamaguchi, M. *et al.* Investigation of annexin A5 as a biomarker for Alzheimer's disease using neuronal cell culture and mouse model. *J. Neurosci. Res.* **88**, 2682–2692 (2010).
33. Cataldo, A. M., Barnett, J. L., Pieroni, C. & Nixon, R. A. Increased neuronal endocytosis and protease delivery to early endosomes in sporadic Alzheimer's disease: neuropathologic evidence for a mechanism of increased beta-amyloidogenesis. *The J. neuroscience: Off. J. Soc. Neurosci.* **17**, 6142–6151 (1997).
34. Nixon, R. A., Yang, D. S. & Lee, J. H. Neurodegenerative lysosomal disorders: a continuum from development to late age. *Autophagy* **4**, 590–599 (2008).
35. Klionsky, D. J. *et al.* Guidelines for the use and interpretation of assays for monitoring autophagy in higher eukaryotes. *Autophagy* **4**, 151–175 (2008).
36. Klionsky, D. J., Cuervo, A. M. & Seglen, P. O. Methods for monitoring autophagy from yeast to human. *Autophagy* **3**, 181–206 (2007).
37. Neniskyte, U., Neher, J. J. & Brown, G. C. Neuronal death induced by nanomolar amyloid beta is mediated by primary phagocytosis of neurons by microglia. *J. Biol. Chem.* **286**, 39904–39913 (2011).
38. Abeti, R. & Abramov, A. Y. Mitochondrial Ca(2+) in neurodegenerative disorders. *Pharmacol. research: Off. J. Italian Pharmacol. Soc.* **99**, 377–381, <https://doi.org/10.1016/j.phrs.2015.05.007> (2015).
39. Abramov, A. Y., Canevari, L. & Duchen, M. R. Beta-amyloid peptides induce mitochondrial dysfunction and oxidative stress in astrocytes and death of neurons through activation of NADPH oxidase. *The J. neuroscience: Off. J. Soc. Neurosci.* **24**, 565–575, <https://doi.org/10.1523/jneurosci.4042-03.2004> (2004).
40. Cederholm, A. & Frostegard, J. Annexin A5 as a novel player in prevention of atherothrombosis in SLE and in the general population. *Ann. N. Y. Acad. Sci.* **1108**, 96–103 (2007).
41. Baek, H. S. *et al.* Annexin A5 suppresses cyclooxygenase-2 expression by downregulating the protein kinase C-zeta-nuclear factor-kappaB signaling pathway in prostate cancer cells. *Oncotarget* **8**, 74263–74275, <https://doi.org/10.18632/oncotarget.19392> (2017).
42. de Jong, R. C. M. *et al.* Annexin A5 reduces infarct size and improves cardiac function after myocardial ischemia-reperfusion injury by suppression of the cardiac inflammatory response. *Sci. Rep.* **8**, 6753, <https://doi.org/10.1038/s41598-018-25143-y> (2018).
43. Stohr, R. *et al.* Annexin A5 reduces early plaque formation in ApoE^{-/-} mice. *PLoS One* **12**, e0190229, <https://doi.org/10.1371/journal.pone.0190229> (2017).
44. Zhang, X. *et al.* Anti-cancer activity of Annexin V in murine melanoma model by suppressing tumor angiogenesis. *Oncotarget* **8**, 42602–42612, <https://doi.org/10.18632/oncotarget.16645> (2017).
45. Kenis, H., Hofstra, L. & Reutelingsperger, C. P. Annexin A5: shifting from a diagnostic towards a therapeutic realm. *Cell. Mol. life sciences: CMLS* **64**, 2859–2862 (2007).
46. van Genderen, H. O., Kenis, H., Hofstra, L., Narula, J. & Reutelingsperger, C. P. Extracellular annexin A5: functions of phosphatidylserine-binding and two-dimensional crystallization. *Biochim. Biophys. Acta* **1783**, 953–963, <https://doi.org/10.1016/j.bbamcr.2008.01.030> (2008).
47. Eberhard, D. A., Brown, M. D. & VandenBerg, S. R. Alterations of annexin expression in pathological neuronal and glial reactions. Immunohistochemical localization of annexins I, II (p36 and p11 subunits), IV, and VI in the human hippocampus. *Am. J. Pathol.* **145**, 640–649 (1994).
48. Cristante, E. *et al.* Identification of an essential endogenous regulator of blood-brain barrier integrity, and its pathological and therapeutic implications. *Proc. Natl Acad. Sci. U S A.* **110**, 832–841 (2013).
49. Kowall, N. W., McKee, A. C., Yankner, B. A. & Beal, M. F. *In vivo* neurotoxicity of beta-amyloid [beta(1-40)] and the beta(25-35) fragment. *Neurobiol. Aging* **13**, 537–542 (1992).
50. Loo, D. T. *et al.* Apoptosis is induced by beta-amyloid in cultured central nervous system neurons. *Proc. Natl Acad. Sci. U S A.* **90**, 7951–7955 (1993).
51. Cotman, C. W., Whittemore, E. R., Watt, J. A., Anderson, A. J. & Loo, D. T. Possible role of apoptosis in Alzheimer's disease. *Ann. N. Y. Acad. Sci.* **747**, 36–49 (1994).
52. Paradis, E., Douillard, H., Koutroumanis, M., Goodyer, C. & LeBlanc, A. Amyloid beta peptide of Alzheimer's disease downregulates Bcl-2 and upregulates bax expression in human neurons. *J. neuroscience: Off. J. Soc. Neurosci.* **16**, 7533–7539 (1996).
53. White, A. R. *et al.* Sublethal concentrations of prion peptide PrP106-126 or the amyloid beta peptide of Alzheimer's disease activates expression of proapoptotic markers in primary cortical neurons. *Neurobiol. Dis.* **8**, 299–316 (2001).
54. Pillai, D. K. *et al.* Directional secretomes reflect polarity-specific functions in an *in vitro* model of human bronchial epithelium. *Am. J. respiratory Cell Mol. Biol.* **50**, 292–300, <https://doi.org/10.1165/rcmb.2013-0188OC> (2014).
55. Calderon, F. & Kim, H. Y. Detection of intracellular phosphatidylserine in living cells. *J. Neurochem.* **104**, 1271–1279, <https://doi.org/10.1111/j.1471-4159.2007.05079.x> (2008).
56. Jaeger, P. A. *et al.* Regulation of amyloid precursor protein processing by the Beclin 1 complex. *PLoS One* **5**, e11102, <https://doi.org/10.1371/journal.pone.0011102> (2010).
57. Nixon, R. A. *et al.* Extensive involvement of autophagy in Alzheimer disease: an immuno-electron microscopy study. *J. neuropathology Exp. Neurol.* **64**, 113–122 (2005).
58. Lipinski, M. M. *et al.* Genome-wide analysis reveals mechanisms modulating autophagy in normal brain aging and in Alzheimer's disease. *Proc. Natl Acad. Sci. U S A.* **107**, 14164–14169, <https://doi.org/10.1073/pnas.1009485107> (2010).
59. Fedeli, C., Filadi, R., Rossi, A., Mammucari, C. & Pizzo, P. PSEN2 (presenilin 2) mutants linked to familial Alzheimer disease impair autophagy by altering Ca(2+) homeostasis. *Autophagy*, 1–19, <https://doi.org/10.1080/15548627.2019.1596489> (2019).
60. Zhang, Z. H. *et al.* Selenomethionine Attenuates the Amyloid-beta Level by Both Inhibiting Amyloid-beta Production and Modulating Autophagy in Neuron-2a/AbetaPPsw Cells. *J. Alzheimers Dis.* **59**, 591–602, <https://doi.org/10.3233/jad-170216> (2017).
61. Nixon, R. A., Cataldo, A. M. & Mathews, P. M. The endosomal-lysosomal system of neurons in Alzheimer's disease pathogenesis: a review. *Neurochem. Res.* **25**, 1161–1172 (2000).
62. Boland, B. *et al.* Autophagy induction and autophagosome clearance in neurons: relationship to autophagic pathology in Alzheimer's disease. *J. neuroscience: Off. J. Soc. Neurosci.* **28**, 6926–6937, <https://doi.org/10.1523/jneurosci.0800-08.2008> (2008).
63. Yu, W. H. *et al.* Macroautophagy—a novel Beta-amyloid peptide-generating pathway activated in Alzheimer's disease. *J. Cell Biol.* **171**, 87–98, <https://doi.org/10.1083/jcb.200505082> (2005).
64. Ghislat, G., Aguado, C. & Knecht, E. Annexin A5 stimulates autophagy and inhibits endocytosis. *J. Cell Sci.* **125**, 92–107, <https://doi.org/10.1242/jcs.086728> (2012).
65. Ditaranto, K., Tekirian, T. L. & Yang, A. J. Lysosomal membrane damage in soluble Abeta-mediated cell death in Alzheimer's disease. *Neurobiol. Dis.* **8**, 19–31, <https://doi.org/10.1006/nbdi.2000.0364> (2001).
66. Oku, Y., Murakami, K., Irie, K., Hoseki, J. & Sakai, Y. Synthesized Abeta42 Caused Intracellular Oxidative Damage, Leading to Cell Death, via Lysosome Rupture. *Cell structure Funct.* **42**, 71–79, <https://doi.org/10.1247/csf.17006> (2017).
67. Nixon, R. A. & Yang, D. S. Autophagy and neuronal cell death in neurological disorders. *Cold Spring Harbor perspectives in biology* **4**, <https://doi.org/10.1101/cshperspect.a008839> (2012).
68. Gordon, P. B., Holen, I., Fosse, M., Rotnes, J. S. & Seglen, P. O. Dependence of hepatocytic autophagy on intracellularly sequestered calcium. *J. Biol. Chem.* **268**, 26107–26112 (1993).
69. Williams, A. *et al.* Novel targets for Huntington's disease in an mTOR-independent autophagy pathway. *Nat. Chem. Biol.* **4**, 295–305, <https://doi.org/10.1038/nchembio.79> (2008).

70. Arispe, N., Rojas, E. & Pollard, H. B. Alzheimer disease amyloid beta protein forms calcium channels in bilayer membranes: blockade by tromethamine and aluminum. *Proc. Natl Acad. Sci. U S Am.* **90**, 567–571 (1993).
71. Abramov, A. Y., Canevari, L. & Duchen, M. R. Changes in intracellular calcium and glutathione in astrocytes as the primary mechanism of amyloid neurotoxicity. *J. neuroscience: Off. J. Soc. Neurosci.* **23**, 5088–5095 (2003).
72. LaFerla, F. M. Calcium dyshomeostasis and intracellular signalling in Alzheimer's disease. *Nat. reviews. Neurosci.* **3**, 862–872 (2002).
73. Viola, K. L. & Klein, W. L. Amyloid beta oligomers in Alzheimer's disease pathogenesis, treatment, and diagnosis. *Acta neuropathologica* **129**, 183–206, <https://doi.org/10.1007/s00401-015-1386-3> (2015).
74. Bhatia, R., Lin, H. & Lal, R. Fresh and globular amyloid beta protein (1–42) induces rapid cellular degeneration: evidence for AbetaP channel-mediated cellular toxicity. *FASEB journal: Off. Publ. Federation Am. Societies Exp. Biol.* **14**, 1233–1243 (2000).
75. Kawahara, M., Kuroda, Y., Arispe, N. & Rojas, E. Alzheimer's beta-amyloid, human islet amylin, and prion protein fragment evoke intracellular free calcium elevations by a common mechanism in a hypothalamic GnRH neuronal cell line. *J. Biol. Chem.* **275**, 14077–14083 (2000).
76. Kuchibhotla, K. V. *et al.* Abeta plaques lead to aberrant regulation of calcium homeostasis *in vivo* resulting in structural and functional disruption of neuronal networks. *Neuron* **59**, 214–225, <https://doi.org/10.1016/j.neuron.2008.06.008> (2008).
77. McKhann, G. M. *et al.* The diagnosis of dementia due to Alzheimer's disease: recommendations from the National Institute on Aging-Alzheimer's Association workgroups on diagnostic guidelines for Alzheimer's disease. *Alzheimer's & dementia: J. Alzheimer's Assoc.* **7**, 263–269, <https://doi.org/10.1016/j.jalz.2011.03.005> (2011).
78. Petersen, R. C. Mild cognitive impairment as a diagnostic entity. *J. Intern. Med.* **256**, 183–194 (2004).
79. Albert, M. S. *et al.* The diagnosis of mild cognitive impairment due to Alzheimer's disease: recommendations from the National Institute on Aging-Alzheimer's Association workgroups on diagnostic guidelines for Alzheimer's disease. *Alzheimer's dementia: J. Alzheimer's Assoc.* **7**, 270–279, <https://doi.org/10.1016/j.jalz.2011.03.008> (2011).
80. Alcolea, D. *et al.* Amyloid precursor protein metabolism and inflammation markers in preclinical Alzheimer disease. *Neurology* **85**, 626–633, <https://doi.org/10.1212/wnl.0000000000001859> (2015).
81. Carro, E., Trejo, J. L., Gomez-Isla, T., LeRoith, D. & Torres-Aleman, I. Serum insulin-like growth factor I regulates brain amyloid-beta levels. *Nat. Med.* **8**, 1390–1397 (2002).
82. Lambert, M. P. *et al.* Diffusible, nonfibrillar ligands derived from Abeta1–42 are potent central nervous system neurotoxins. *Proc. Natl Acad. Sci. U S Am.* **95**, 6448–6453 (1998).
83. Bartolome, F. *et al.* Pathogenic p62/SQSTM1 mutations impair energy metabolism through limitation of mitochondrial substrates. *Sci. Rep.* **7**, 1666, <https://doi.org/10.1038/s41598-017-01678-4> (2017).

Acknowledgements

We are grateful to the patients and donors without which these work would not have been possible. Also, we thank Dr. Marife Cano who kindly helped us to obtain and perform choroid plexus cell cultures. This study was supported by grants from the *Instituto de Salud Carlos III* (FIS2015/00780, PI18/00118), FEDER, joint grant from Comunidad de Madrid (S2017/BMD-3700; NEUROMETAB-CM), *Fundación Ramón Areces* (CIVP16A1825), and *CIBERNED* (PI2016/01). Part of the work was supported by the NIHR Queen Square Dementia Biomedical Research Unit. This work was undertaken at UCLH/UCL which receives a proportion of funding from the Department of Health's NIHR Biomedical Research Centres funding scheme.

Author contributions

F.B. and E.C. were responsible for experimental designs, data interpretation and writing of the paper. F.B., A.K., M.C., C.P. and D.A. performed and analysed the experiments. C.S., A.V.G., A.R., J.F., D.A., A.L.L. and I.F. provided human samples. J.H. and A.Y.A. contributed feedback the manuscript. J.H., A.Y.A. and E.C. obtained the funding. All authors reviewed and corrected the manuscript.

Competing interests

The authors declare no competing interests.

Additional information

Supplementary information is available for this paper at <https://doi.org/10.1038/s41598-020-66177-5>.

Correspondence and requests for materials should be addressed to F.B. or E.C.

Reprints and permissions information is available at www.nature.com/reprints.

Publisher's note Springer Nature remains neutral with regard to jurisdictional claims in published maps and institutional affiliations.



Open Access This article is licensed under a Creative Commons Attribution 4.0 International License, which permits use, sharing, adaptation, distribution and reproduction in any medium or format, as long as you give appropriate credit to the original author(s) and the source, provide a link to the Creative Commons license, and indicate if changes were made. The images or other third party material in this article are included in the article's Creative Commons license, unless indicated otherwise in a credit line to the material. If material is not included in the article's Creative Commons license and your intended use is not permitted by statutory regulation or exceeds the permitted use, you will need to obtain permission directly from the copyright holder. To view a copy of this license, visit <http://creativecommons.org/licenses/by/4.0/>.

© The Author(s) 2020